Theor Chem Acc (2012) 131:1185
DOI 10.1007/s00214-012-1185-z

REGULAR ARTICLE

Giant correlation effects in the photoelectron spectrum of $Ni(C_3H_5)_2$: clues from accurate calculation of ionization cross-sections

P. Decleva · G. Fronzoni · M. Stener

Received: 21 July 2011 / Accepted: 14 December 2011 / Published online: 10 March 2012

Abstract Several general issues relating to the strong correlation effects present in the ionic states and the interpretation of molecular photoelectron spectra are discussed in the context of the $Ni(C_3H_5)_2$ molecule, and the problematic assignment of its spectrum is considered. Accurate calculations of photoionization cross-sections relative to all the valence ionizations are computed and compared with the available experimental evidence. It is shown that most ambiguities are resolved by a careful analysis of cross-section profiles and branching ratios, which reveal a wealth of details on the complex electronic structure of this molecule.

Keywords Photoelectron spectroscopy · Time-dependent density functional theory · Transition metal compounds · Correlation effects

1 Introduction

The accurate description of correlation effects in transition metal compounds has remained an important challenge for theoretical approaches [1, 2]. In the domain of ab initio methods such effects are often unusually large, especially for excited and ionized states relevant to spectroscopy. The situation is much alleviated with DFT approaches, which are able to better describe the differential correlation associated with metal d electrons [3]. However, in close situations, the accuracy of present DFT approaches may not be sufficient to give an unambiguous answer, and one has to resort to pushing ab initio approaches to a high level of correlation.

One of the most direct probes of the electronic structure is the measurement of ionization potentials by photoelectron spectroscopy. In fact since the earliest studies, it has become apparent that huge deviation from the predictions of Koopmans Theorem (KT), which often works reasonably well for main group elements, occur in organometallic compounds, although by no means always, and the origin of this widely varying behavior is not well understood. Actually one of the first and most simple systems investigated, the nickel bis (π-allyl) molecule [$Ni(\eta^3$–$C_3H_5)_2$] [4], has proved one of the most difficult examples, revealing successive layers of complexity, so that it is still not completely understood. Besides comparison with similar compounds, a decisive clue to the assignment of the spectrum, and in particular, to the nature of the outermost ionization, has been provided by cross-sections and branching ratios (BR) profiles obtained with synchrotron radiation [5, 6], which have supplemented earlier suggestions originating from HeI/HeII intensity variations [4, 7], eliminating all the ambiguity inherent in previous studies, like accidental ratios due to the many non-monotonic features present in molecular cross-sections, like delayed onsets, shape and autoionization resonances, Cooper minima, further multi-electron excitations [8–10]. Unfortunately, at the time of the experimental studies, only rather primitive theoretical approaches were available (basically

Dedicated to Professor Vincenzo Barone and published as part of the special collection of articles celebrating his 60th birthday.

P. Decleva · G. Fronzoni · M. Stener (✉)
Dipartimento di Scienze Chimiche, Università di Trieste,
Via L. Giorgieri 1, 34127 Trieste, Italy
e-mail: stener@univ.trieste.it

P. Decleva · G. Fronzoni · M. Stener
Consorzio Interuniversitario Nazionale per la Scienza e Tecnologia dei Materiali, Unita' di Trieste and CNR-IOM DEMOCRITOS, Trieste, Italy

the Gelius model [11] and the MS-Xα approach [12–14]) to supplement and interpret the experimental data, for molecules of such complexity. Since then significant advances have been made in the calculation of molecular cross-sections, and it is presently feasible to compute full TDDFT continuum properties of organometallic compounds obtaining convergent results without further approximations [15–17].

As a contribution to the clarification of the electronic structure of this deceptively simple prototypical system, we have undertaken a TDDFT calculation of the photoionization parameters, to check the consistency and interpretation of the SR data, gaining further evidence and confirmation of the assignment of the spectrum and the sequence of ionization potentials. Additional interest comes to the clarification of the possible occurrence of resonances, and in particular, the characterization of the expected "giant resonance" associated with the 3p → 3d excitation in the metal center [18], which has hitherto escaped experimental detection. Moreover, it is expected that finer details revealed by improved theoretical description may stimulate further experimental investigations of photoionization parameters, both angular distributions, hitherto neglected and cross-sections with the much improved resolution and wider energy range now currently available, which could shed light on the most difficult details of the ordering of the outermost ionizations, still not unambiguously settled. At the same time, the challenge of an accurate description of the electronic structure of this basic organometallic compound and its lower ionic states, notably the characterization of the HOMO, should give a stringent test of the accuracy of the most highly correlated approaches presently available.

2 Theoretical method

In this work, we have employed the non-iterative TDDFT B-spline LCAO formalism for the calculation of the continuum. The formalism, its implementations and the numerical details are fully described in [16], and will be summarized here.

A conventional ground state calculation is first performed, employing the ADF program [19]. Then the KS (Kohn–Sham) hamiltonian matrix is calculated, employing the LCAO B-spline basis set. Occupied orbitals are then obtained as bound eigenvectors:

$$H_{\mathrm{KS}}\varphi_i = \varepsilon_i\varphi_i \quad i = 1,\ldots,n.$$

While continuum photoelectron orbitals are extracted as eigenvectors with minimum modulus eigenvalue of the energy-dependent matrix $\mathbf{A}^{+}\mathbf{A}$:

$$\mathbf{A}^{+}\mathbf{A}(E)c = ac, \quad \mathbf{A}(E) = \mathbf{H} - E\mathbf{S}$$

where $\mathbf{H}$ and $\mathbf{S}$ are the Hamiltonian and overlap matrices, respectively, E is the photoelectron kinetic energy, c the eigenvectors and a the minimum modulus eigenvalues. In the TDDFT formalism, the linear response of an electronic density to an external time-dependent electromagnetic field with frequency ω is evaluated following the original scheme of Zangwill and Soven [20]; an effective Self-Consistent Field (SCF) potential Φ^{SCF} is introduced, which consists of the external dipole potential Φ^{EXT} plus the Coulomb and exchange correlation screening due to the first-order change in the electron density $\delta\rho$ induced by the field

$$\delta\rho = \chi(\omega)\,\Phi^{\mathrm{SCF}}$$

$$\delta\Phi = K\,\delta\rho \quad \Phi^{\mathrm{SCF}} = \Phi^{\mathrm{EXT}} + \delta\Phi$$

Here $\chi(\omega)$ is the frequency-dependent electric susceptibility and K the linear response of the field to a density perturbation. Together they afford a linear equation for the effective potential Φ^{SCF}

$$(K\chi - 1)\,\Phi^{\mathrm{SCF}} = -\Phi^{\mathrm{EXT}}$$

Representing the functional equation with the same B-spline LCAO basis set leads to the solution of a linear system of algebraic equations. Once Φ^{SCF} is obtained, all the parameters that describe the photoionization process, namely the cross-section and the asymmetry parameters, are calculated via transition moments using Φ^{SCF} instead of dipole operator. Introducing an additional subscript λ_{r} to distinguish among the three dipole components that transform like the standard spherical harmonics with $l = 1$ and $\mathrm{m} = \lambda_r$, that is, $\Phi^{\mathrm{EXT}}_{\lambda_r}(\bar{r},\omega) = \sqrt{\frac{4\pi}{3}} r Y_{1,\lambda_r}$. The dipole transition moments are finally obtained, employing the $\Phi^{\mathrm{SCF}}_{\lambda_r}$ potential instead of the dipole operator:

$$D^{\lambda\mu-}_{lh}(\lambda_r) = \left\langle \varphi^{\lambda\mu-}_{lh} \middle| \Phi^{\mathrm{SCF}}_{\lambda_r} | \varphi_i \right\rangle,$$

where φ_i is the one-electron KS orbital, which is currently ionized, and $\varphi^{\lambda\mu-}_{lh}$ is the continuum solution for channel lh in final symmetry $\lambda\mu$, normalized to incoming wave asymptotic boundary condition.

A DZP basis set of Slater type orbitals (TZP for Ni), taken from the ADF database [19], has been employed in the initial SCF calculation. The B-spline basis [15] employed in subsequent calculation is defined by the radial interval [0, 20] a.u., with step 0.2 a.u. and maximum angular expansion up to $L = 16$, supplemented by short expansions around the nuclei, with maximum $L = 2$ for C and $L = 1$ for H. Convergence tests at the DFT level have shown that the basis employed is completely convergent up to 2.5 a.u. electron kinetic energy, covering the

entire range reported. LB94 exchange correlation potential [21] has been employed in H_{KS}, while the exchange correlation kernel in the TDDFT response equation has been approximated at the ALDA level [22].

3 Results and discussion

A qualitative orbital scheme, as obtained by the present DFT calculation, relative to $Ni(C_3H_5)_2$ and the two separate fragments, $(C_3H_5)_2$ and Ni ($3d^9 4$ s), is reported in Fig. 1. Metal d orbitals (percentage of d contribution in parenthesis) are $13a_g$ (75%, mostly d_{xy}), $12a_g$ (90%, d_{x2-y2}), $11a_g$ (87%, d_{z2}), $6b_g$ (85%, 54% d_{yz} + 34% d_{xz}), $5b_g$ (57%, 34%d_{yz} + 23% d_{xz}). Moreover, 15% of d_{xy} and d_{xz} are in $9a_g$ and $4b_g$, respectively. A HeI photoelectron spectrum of the outer valence ionization is shown in Fig. 2 (from Ref. [7]). The 9 bands resolved (actually the next band at 17.9 eV is also weakly apparent), together with the three following bands, revealed in the SR study [6], comprise 22 main

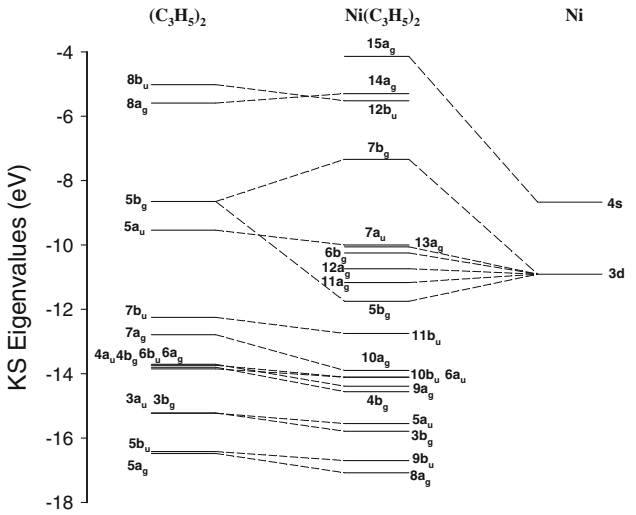

Fig. 1 Outer valence molecular orbital *diagram* for $Ni(C_3H_5)_2$ from *eigenvalues* of present ground state DFT calculation

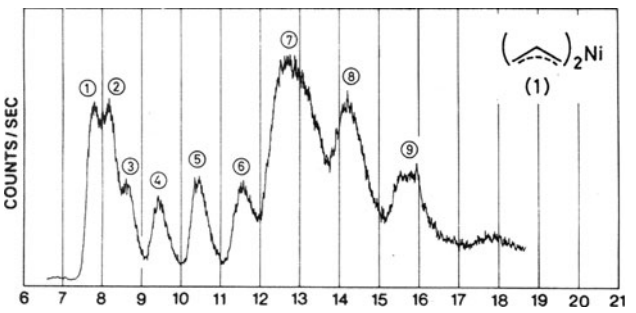

Fig. 2 He I photoelectron spectrum of $Ni(C_3H_5)_2$. Adapted with permission from Ref. [7]. Copyright (1976) American Chemical Society

ionizations, so several bands are composite. Actually the spectrum separates neatly into 3 regions. The first, comprising bands 1–4, are attributed to the mainly Ni 3d molecular orbitals (11–13 a_g, 5–6 b_g) and the highest π orbital of the allyl moiety, $7a_u$. Bands 5 ($11b_u$) and 6 ($10a_g$) are the ionizations due to the remaining two allyl π orbitals, while the remaining bands comprise the allyl σ ionizations. The assignment is by no means unambiguous and will be discussed below. A summary of different proposals and theoretical results is reported in Table 1.

As already mentioned, the interest in the electronic structure and ionization energies of $Ni(C_3H_5)_2$ was spurred by the strong disagreement between experimental evidence and the results of Hartree–Fock (HF) calculations [1, 23], that is, the huge breakdown of the Koopmans Theorem [24]. This is primarily due to very large relaxation effects, about 10 eV, for the metal d ionizations, which are buried deep in the valence shell at the HF level, but are assigned to the outermost ionizations (bands 1–4) on experimental grounds. Apart from relaxation, additional correlation effects, notably strong correlation within the 3d shell, and differential correlation between metal 3d and ligand orbitals come into play, so that even highly correlated calculations [25–28] have proved inadequate for a clear-cut assignment of the spectrum. In particular, already the nature of the HOMO ionization has been debated, with most calculations (as well as comparison with Pd and Pt analogues) favoured assignment to the allyl π orbital [25, 26, 28–32], while one of the first careful experimental analysis [7], later amply confirmed by a synchrotron radiation study [5, 6], assign it to metal d ionization.

An important issue regards also the nature of the orbital being ionized. Due to the large relaxation and additional correlation effects, the nature of the orbitals change dramatically upon ionization, as all ab initio calculations have clearly indicated [25–28, 32]. This renders essentially useless the use of canonical HF orbitals to describe ionization and has broad implications about describing molecular properties and reactivity in terms of HF HOMO, in such compounds. In fact, it is the Dyson orbital:

$$\varphi_I(\mathbf{x}) = \int \Psi_I^*(\mathbf{x}_2, \ldots, \mathbf{x}_N)\Psi_0(\mathbf{x}, \mathbf{x}_2, \ldots, \mathbf{x}_N)\mathrm{d}\mathbf{x}_2 \ldots \mathrm{d}\mathbf{x}_N$$

which is well defined, as a transition property between the initial neutral and the final ionic state, Ψ_0 and Ψ_I, respectively, and does not rely on any specific form of the initial and final wave functions. Note also that it is the Dyson orbital, which is in principle observable, for instance, by electron momentum spectroscopy [33], or the imaging techniques recently developing from high harmonic generation or ionization yields with strong IR laser pulses [34, 35]. In any case, also ionization cross-sections are basically described as dipole transitions from the Dyson

Table 1 IP values (eV) and assignments of the valence photoelectron spectrum of $Ni(C_3H_5)_2$

Band	Experiment			Theory					
	IP[a]	IP[b]	Assignment[a]	Ref.[c,d]	2ph-TDA	CI	2 h-1p	4 h-3v-2p	LB94
1	7.76	7.64/7.79	d + d	$7a_u$	$7a_u$	$13a_g$, $6b_g$	$13a_g$, $5b_g$	$7a_u$	$7a_u$, $13a_g$
2	8.19	7.95/8.15	$7a_u$ (π) + d	$12a_g$, $5b_g$, $13a_g$	$13a_g$, $6b_g$	$7a_u$	$11a_g$, $10a_g$	$13a_g$, $5b_g$	$6b_g$, $12a_g$
3	8.58	8.52	d	$11a_g$	$11a_g$, $5b_g$		$7a_u$	$11a_g$, $10a_g$	$11a_g$
4	9.40	9.38	d_{xz} (b_g)	$6b_g$	$10a_g$		$6b_g$	$6b_g$	$5b_g$
5	10.38	10.36	b_u (π)	$11b_u$	$11b_u$		$11b_u$	$11b_u$	$11b_u$
6	11.55	11.48	a_g (π)	a_g (π + d)	$9a_g$			$9a_g$	$10a_g$
7	12.7	12.6	a_g + b_u (σ)	$6a_u$, $10b_u$, $12a_g$, $4b_g$	$6a_u$, $10b_u$, $12a_g$, $4b_g$				$6a_u$, $10b_u$, $9a_g$, $4b_g$
8	14.2	14.2	b_g + a_u (σ)		$5a_u$, $3b_g$				$5a_u$, $3b_g$
9	15.6	15.6			$9b_u$, $8a_g$				$8a_g$, $9b_u$
10		17.9							$7a_g$, $8b_u$
11		20.8							$4a_u$, $2b_g$
12		24.0							$6a_g$, $7b_u$

[a] Ref. [7]

[b] Ref. [6]

[c] Ref. [28]

[d] Ref. [30]

orbital to the photoelectron continuum and can therefore afford a clear signature of the difference between the different descriptions. It is remarkable that in cases where HF and Dyson orbitals are very different, DFT Kohn–Sham orbitals appear much closer to the latter, underlying a deep difference between the two, which has not been adequately investigated.

With all these caveats, the computed cross-sections at the TDDFT level will be presently discussed.

A strong important clue to the assignment of the metal d ionizations as distinct from the ligand ones is the behavior of the cross-section. MOs derived from 2p orbitals of the first row atoms show cross-sections that decay much faster than those derived from metal 3d AO's, although they are larger at low energy [8–10]. It is well exemplified in the computed cross-section data of the $13a_g$–$9a_g$ orbitals reported in Fig. 3. $13a_g$–$11a_g$ are predominantly metal 3d, while $10a_g$ and $9a_g$ are essentially ligand orbitals. This has been successfully employed already in the earlier HeI/HeII studies [7] and is confirmed much more clearly with the SR studies [5, 6]. This information alone strongly supports the attribution of the metal d ionizations to the first four experimental bands in the photoelectron spectrum. All calculations agree in placing the allyl π ionization $7a_u$ among the outermost ones, so that it is also firmly comprised in the same experimental bands. Moreover, all calculations as well as qualitative arguments place immediately below the two orbitals deriving from the first allyl π orbital. Therefore, also on intensity grounds, bands

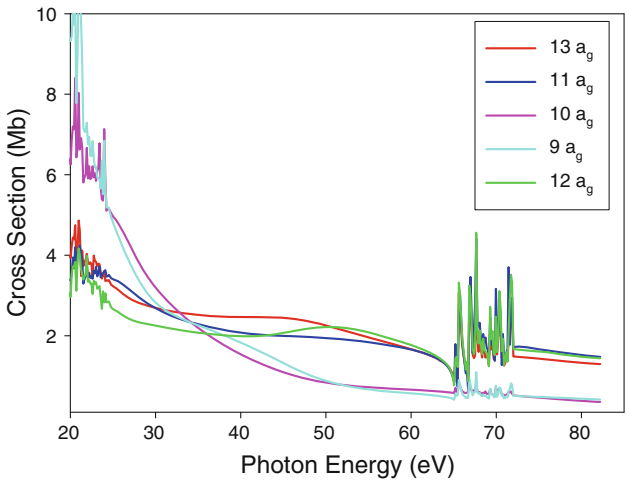

Fig. 3 Calculated cross-sections for the valence orbitals of a_g symmetry of $Ni(C_3H_5)_2$, $9a_g$–$13a_g$

5 and 6 are attributed to the individual $11b_u$ and $10a_g$ π allyl orbitals, and the following bands, 7–9 to allyl σ orbitals (including bands 10–12, the latter two being "inner valence" ionizations, mainly derived from carbon 2 s AO's). So the high energy part of the spectrum appears rather straightforward, with 4 ionizations ($6a_u$, $10b_u$, $9a_g$, $4b_g$) attributed to band 7, both on intensity grounds and on general agreement with theoretical ionization energies, followed by closely spaced couples, deriving from symmetric and antisymmetric combinations of individual allyl orbitals, either (a_u, b_g) or (a_g, b_u): bands 8 to $5a_u$, $3b_g$

ionizations, bands 9 to $8a_g$ and $9b_u$, bands 10 to $7a_g$, $8b_u$, bands 11 to $4a_u$, $2b_g$ and bands 12 to $6a_g$ and $7b_u$.

4 Ligand bands

The branching ratios of the ligand bands 5–9 are reported in Fig. 4. They are clearly proportional to the number of single ionizations under each band, 1 for bands 5–6, 2 for bands 8–9, 4 for band 7, giving a neat evidence for this assignment. One can observe a much larger contribution of the 3p → 3d resonance in band 7, a clear indication of some metal 3d contribution to these states. Moreover, from individual cross-sections reported in Fig. 5, it appears that this contribution is dominated by that of $9a_g$ and $4b_g$ ionizations, as it is expected on symmetry grounds. The d participation leads also to a distinct increase in cross-section for these two ionizations in comparison with the other two, $6a_u$ and $10b_u$, at high energy, because of the larger d atomic cross-section. The resonances are, however, weakly present in all channels, even though symmetry forbids d participation, so that rather strong interchannel coupling is active in this case.

A second feature superimposed to the general decreasing behavior of the cross-sections is the presence of oscillations that give rise to large-scale structures, sufficiently strong that they can be observable, giving therefore a precise characterization of the individual ionizations. As an example, bands 5 and 6 which both derive from the ionization of two very similar orbitals, the even and odd combinations of the 1π orbital of the allyl molecule, $11b_u = \pi_+$ and $10a_g = \pi_-$, show a strong oscillation in their respective cross-sections, which is even more clearly apparent taking their ratio, reported in Fig. 6. The similarity with the analogous oscillations well known in C_{60} [36, 37] and $MgCp_2$ [38] definitely point to their attribution to interference phenomena due to coherent emission from equivalent centers, in their case from the two 1π orbitals on the two allyl fragments, with opposite phase for the π_u and π_g combinations. Oscillations are present also in the remaining bands, notably with doubled frequency for the bands 8 and 9, although with smaller amplitude. This is because of the interplay of two overlapped ionizations within each experimental band.

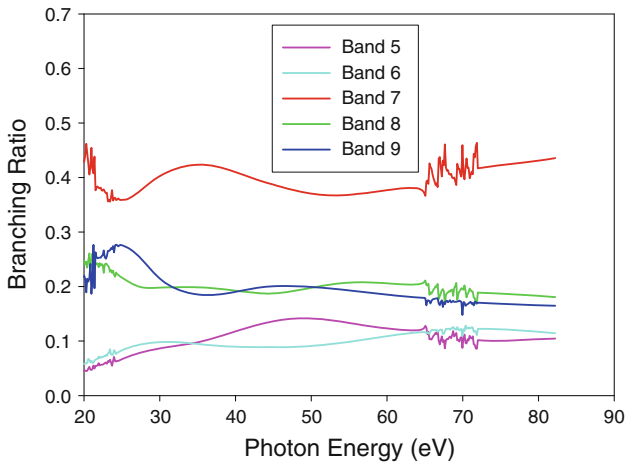

Fig. 4 Calculated branching ratios for the ligand photoelectron bands (bands 5–9)

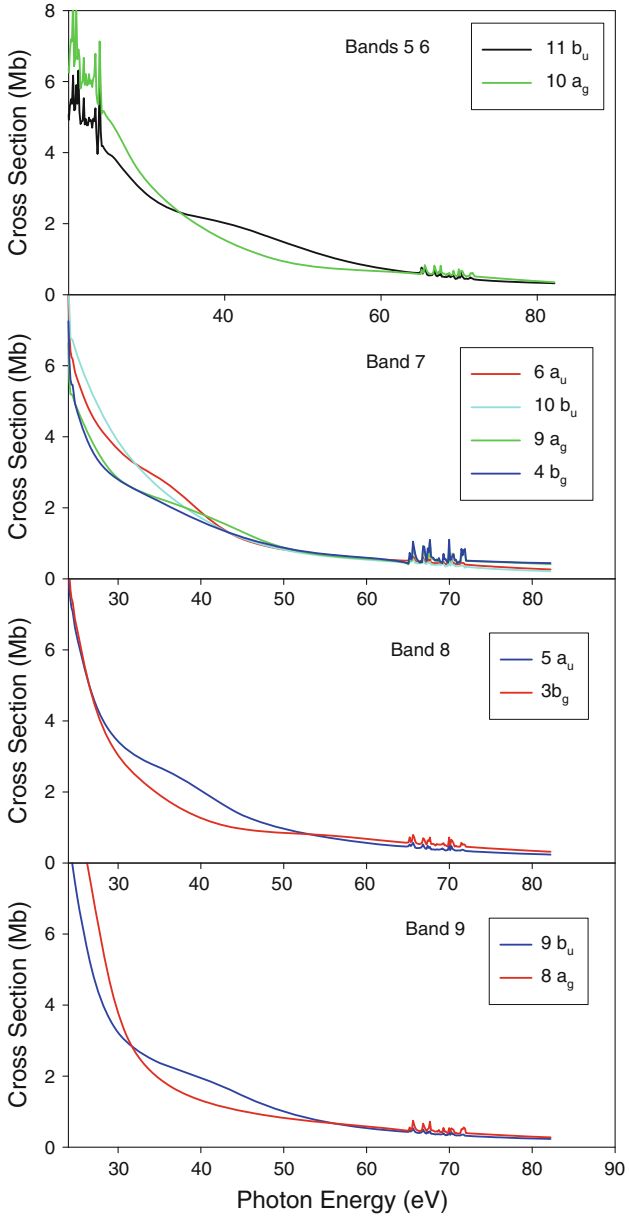

Fig. 5 Cross-sections for individual ionizations comprising the ligand bands, from *upper to lower panel*: *bands 5* ($11b_u$) and *6* ($10a_g$); *band 7* ($6a_u$, $10b_u$, $9a_g$, $4b_g$); *band 8* ($5a_u$, $3b_g$); *band 9* ($8a_g$, $9b_u$)

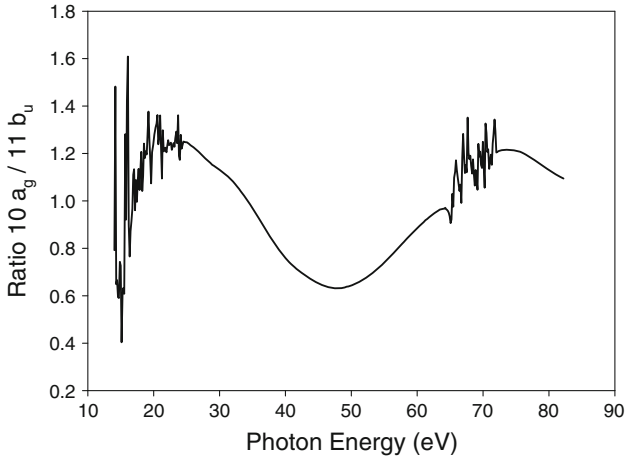

Fig. 6 Cross-section ratio of the $10a_g$ to $11b_u$ ionization (*band 6 to band 5*)

5 Bands 1–4

A first problem is the assignment of band 4, which on intensity grounds is attributed to a single ionization, with metal d character. In fact, assignment to the $7a_u$ (π) ionization is easily discarded, both on the basis of computed ionization potentials, which give a much larger separation with the other π ionizations (bands 5 and 6) and on the intensity ratios at high energy. The experimental ratio [5, 6] between bands 4 and 5 at $h\nu = 80$ eV is around 2, which is by far too large to attribute the $7a_u$ ionization to band 4. The two metal d orbitals available at higher energy are $11a_g$ and $5b_g$, and their calculated ratio to $11b_u$ in band 5 is shown in Fig. 7. As can be seen their ratio is similar up to about $h\nu = 50$ eV, but diverges strongly at high energy past the 3p $\rightarrow$ 3d resonance region, around $h\nu \sim 70$–80 eV. Here the ratio of the $5b_g$ ionization is a little larger than 2 and that relative to $11a_g$ becomes closer to 4. This is partially due to the lower Ni 3d content of $5b_g$, which is the orbital mostly involved in the back bonding toward the π^* ($7b_g$) orbital of the bis-allyl fragment, which also explains the lowering in energy of this orbital with respect to the other Ni 3d-derived ionizations. Again this ratio gives a strong support for the attribution of the $5b_g$ ionization to band 4, as several previous studies have suggested [7, 27–31], although the high level ab initio 2ph TDA approach gives the reverse assignment to 11 a_g [25, 26, 32]. The most difficult part is the assignment of bands 1–3. As already mentioned, they should comprise 5 ionizations, four mainly metal d orbitals, $11a_g$–$13a_g$ and $6b_g$, and the $7a_u$ π allyl orbital. The relative cross-sections are reported in Fig. 8. Again the much faster decrease in $7a_u$ cross-section compared to that of metal 3d ionizations is apparent. It is about 50% larger close to threshold, and it becomes lower by a factor of 5 at 80 eV. At this energy, the spread of metal 3d ionizations varies from 1.325 Mb for $13a_g$ to 1.648 Mb for $6b_g$. The attribution of the first peak to the $7a_u$ ionization, favored by most of the latter studies [25–32], comprising some of the highest level ab initio calculations is therefore completely untenable, as pointed out by the SR study [5, 6].

Again the behavior of the experimental intensities at high energies [5, 6], $\sigma 1 > \sigma 2 > \sigma 3$, but of similar magnitudes, suggests the attribution of two metal d ionizations to the first band, 1 metal d + $7a_u$ to the second and 1 metal d to the third.

In fact the intensity ratios exclude the assignment of the $7a_u$ alone to any band (Fig. 9). Moreover, branching ratios associating $7a_u$ with one metal d ionization invariably show σ (2 metal d) > σ (1 metal d + 7au) > σ (1 metal d), so that the only sensible assignment is two metal d ionizations to the first band, 1 metal d + $7a_u$ to the second and 1 metal d to the third.

Individual assignment is more difficult.

The third band should be attributed either to $11a_g$ or to $6b_g$. That leaves the three possibilities for the first three bands:

(a) ($13a_g$, $12a_g$), ($6b_g$, $7a_u$), $11a_g$
(b) ($13a_g$, $6b_g$), ($12a_g$, $7a_u$), $11a_g$
(c) ($13a_g$, $12a_g$), ($11a_g$, $7a_u$), $6b_g$

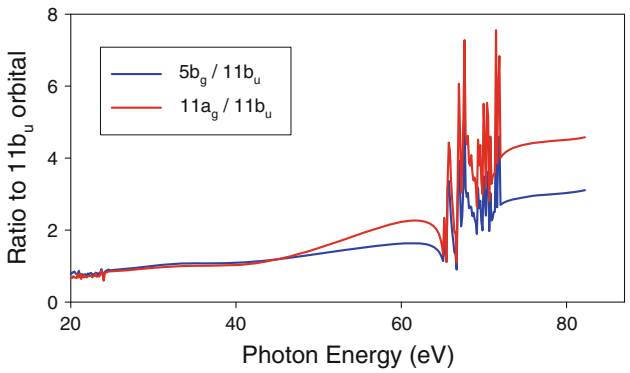

Fig. 7 Cross-section ratio of the $11a_g$ and $5b_g$ to $11b_u$ ionization

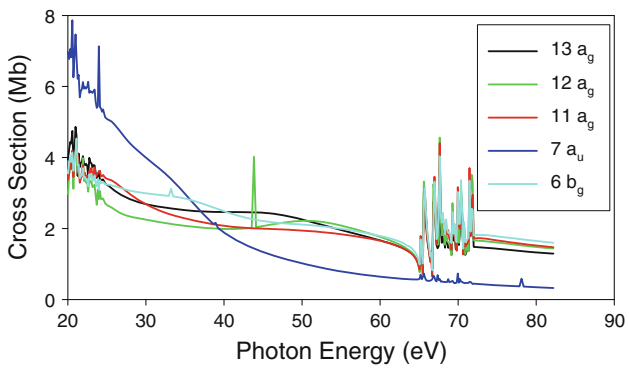

Fig. 8 Cross-sections for the ionizations comprised in the three outermost *bands*: $11a_g$–$13a_g$, $6b_g$, $7a_u$

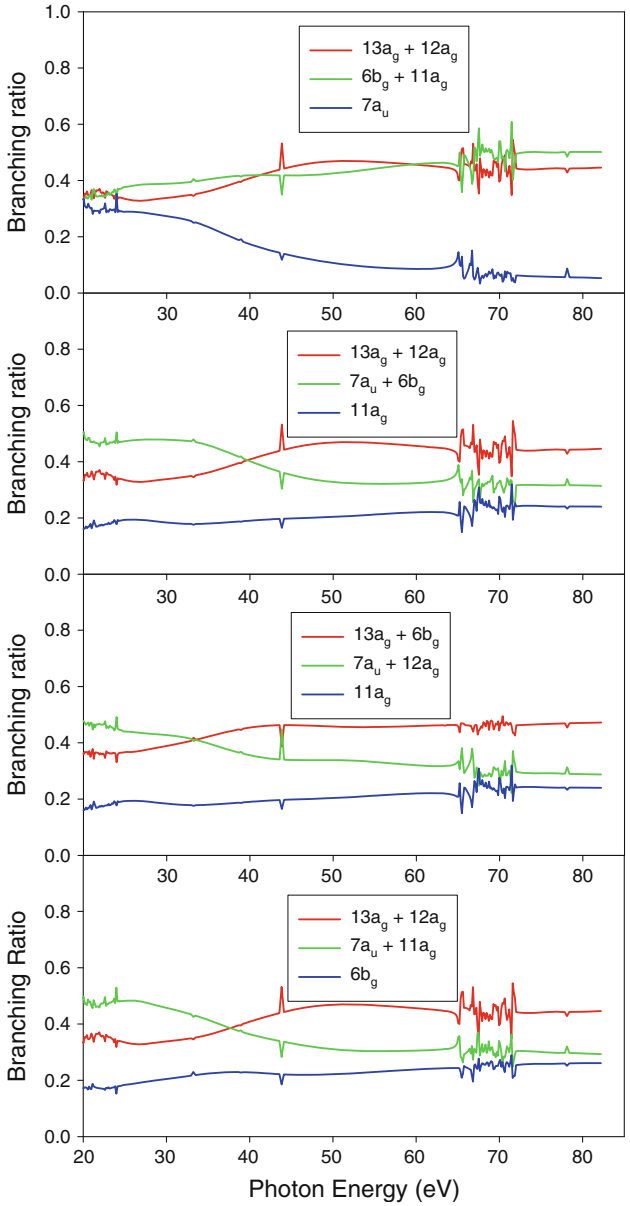

Fig. 9 Branching ratios relative to different possible assignments for the three outermost bands, see text for discussion

The relevant branching ratios, together with one BR relative to $7a_u$ considered alone, are reported in Fig. 9.

It will be probably hard to distinguish experimentally between the three possibilities, not to mention inadequacies of the theoretical results in comparison with experiment. One may only point out that assignment (a) leads to a significantly more even distribution of relative intensities at high energy, which appear quantitatively more in line with the experimental results available [5, 6], while the other two, especially (c), give a first peak intensity much larger than the other two, with a small difference between the second and the third.

A possible significant feature of assignment (b) is the much reduced amplitude of the 3p → 3d resonant structure in the first BR, compared to that of the other two. Possible additional information could come from the behavior of the cross-sections at still higher energies, or the angular distributions, in particular for band 3 which could distinguish between $11a_g$ and $6b_g$ ionizations, or more exotic techniques, like photoionization from the oriented molecule [39, 40]. Also a very high-resolution study may be able to further slice bands 1–3, as suggested from high-resolution spectra reported in Ref. [6], and possibly give the full ordering of ionizations within the first three bands.

Moreover, investigation of geometry dependence [41] and the possible presence of the cis conformer [42] have to be assessed.

At the present stage, assignment (a) seems slightly more favored, which is in complete agreement with that of the last SR study [6]. It is remarkable, however, how by a careful consideration of cross-sections alone a rather complete and firm assignment of this difficult spectrum can be achieved, the only ambiguity being confined to the three possibilities just considered for the three outermost bands.

Finally, it is interesting to point out the remarkably low intensity of the 3p → 3d resonance peaks in this region. A comparison of total cross-section for $Ni(C_3H_5)_2$ with that for $Ni(CO)_4$ is reported in Fig. 10. A striking difference is apparent. While in $Ni(CO)_4$, the spectrum shows a single large-intensity Fano profile with weak Rydberg-like structures superimposed in $Ni(C_3H_5)_2$, the large structure is absent while low intensity peaks are distributed over the whole resonant region. This indicates that a single virtual orbital carries most of the available 3d content, which is sizable, in the former molecule, while little 3d participation is available in the virtual space of $Ni(C_3H_5)_2$, and it is distributed over several virtual states. That is a clear

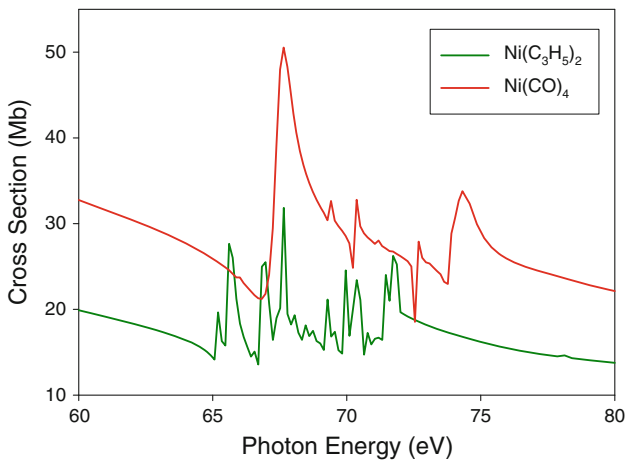

Fig. 10 Total ionization cross-section for $Ni(C_3H_5)_2$ and $Ni(CO)_4$ in the region of the 3p → 3d resonance

indication of the rather weak back bonding in $Ni(C_3H_5)_2$, which has a metal configuration closer to $3d^{10}$, while a much stronger backbonding is present in $Ni(CO)_4$, which is in fact a very stable system, pushing a significant 3d component in the corresponding antibonding orbital.

6 Conclusions

The $Ni(C_3H_5)_2$ molecule is a remarkable compound, a model for organometallic chemistry and olefine transition metal bonding, which despite its apparent simplicity shows a very complex electronic structure, dominated by strong correlation effects. It represents therefore a prototypical molecule for the study of electron correlation in transition metal compounds, and of the theoretical approaches to the computation of ionization potentials. Not only is the sequence of ionization energies widely different from that afforded by HF eigenvalues, but notably the Dyson orbitals, physically associated with the various final ionic states, are much different from the canonical HF orbitals, which challenge the use of such orbitals for the description of the electronic structure, and in particular of the HF HOMO in discussing chemical properties and reactivity in this class of molecules.

On the contrary, it appears that DFT has the ability to give orbitals much closer to Dyson than to HF in cases where their difference is large, notably in transition metal compounds [43], a remarkable property that remains to be further investigated.

In this context, the study of dynamical photoionization properties, cross-sections and possibly angular distributions give substantial and unique information on the electronic structure of such compounds, yielding a precise characterization of the orbitals associated with the various ionizations, and in particular, strong clues for the assignment of difficult spectra. It is remarkable that despite the additional complexities involved in the calculation of molecular continuum states and photoionization cross-sections with respect to the calculation of bound states, it appears easier to obtain reliable photoionization parameters than ionization energies accurate enough to resolve ambiguous assignments, when bound state correlation effects are so complex as in this system.

Finally, it must be stressed that several issues remain open in the present case: The role of geometry and the possible presence and contribution of the cis conformer, the push of highly correlated ab initio techniques to obtain convergent results for the correct sequence of final ionic states, a challenge for current ab initio approaches, and on the experimental side, a more accurate characterization of the photoionization parameters, including angular distributions and over a larger energy range, exploiting the much higher fluxes and energy resolution presently available at SR facilities.

Acknowledgments A generous amount of computer time at CINECA through ISCRA B project TRAMCREP "Transition metal compounds: resonances in photoionization" is gratefully acknowledged.

References

1. Veillard A, Demuynck J (1977) In: Schaefer HF (ed) Modern theoretical chemistry, vol 4. Plenum Press, New York, p 187
2. Neese F, Petrenko T, Ganyushin D, Olbrich G (2007) Coord Chem Rev 251:288
3. Decleva P, Fronzoni G, Lisini A (1991) In: Labanowski JK, Andzelm JW (eds) Density functional methods in chemistry. Springer, New York, p 323
4. Lloyd and DR, Lynaugh N (1972) In: Shirley DE (ed) Electron spectroscopy. North-Holland, Amsterdam, p 445
5. Li X, Bancroft GM, Puddephatt RJ, Hu YF, Liu Z, Tan KH (1992) Inorg Chem 31:5162
6. Li X, Bancroft GM, Puddephatt RJ, Liu ZF, Hu YF, Tan KH (1994) J Am Chem Soc 116:9543
7. Batich CD (1976) J Am Chem Soc 98:7585
8. Green JC (1994) Acc Chem Res 27:131
9. Li X, Bancroft GM, Puddephatt RJ (1997) Acc Chem Res 30:213
10. Green JC, Decleva P (2005) Coord Chem Rev 249:209
11. Gelius U, Siegbahn K (1972) Faraday discuss. Chem Soc 54:257
12. Dill D, Dehmer JL (1974) J Chem Phys 64:692
13. Dehmer JL, Dill D (1979) In: Rescigno T, McKoy V, Schneider B (eds) Electron-molecule and photon-molecule collisions. Plenum, New York, p 225
14. Chermette H (1992) New J Chem 16:1081
15. Toffoli D, Stener M, Fronzoni G, Decleva P (2002) Chem Phys 276:25
16. Stener M, Fronzoni G, Decleva P (2005) J Chem Phys 122:234301
17. Stener M, Fronzoni G, Decleva P (2009) Chem Phys 361:49
18. Martins M, Godehusen K, Richter T, Wernet P, Zimmermann P (2006) J Phys B: At Mol Opt Phys 39:R79
19. Fonseca Guerra C, Snijders JG, te Velde G, Baerends EJ (1998) Theor Chem Acc 99:391
20. Zangwill A, Soven P (1980) Phys Rev A 21:1561
21. Van Leeuwen R, Baerends EJ (1994) Phys Rev A 49:2421
22. Gross EKU, Kohn W (1990) Adv Quantum Chem 21:255
23. Rohmer MM, Demuynck J, Veillard A (1974) Theor Chim Acta 36:93
24. Cederbaum LS, Domcke W, Schirmer J, von Niessen W (1986) Adv Chem Phys 65:115
25. Moncrieff D, Hillier IH, Saunders VR, von Niessen W (1985) J Chem Soc Chem Commun 779
26. Moncrieff D, Hillier IH, Saunders VR, von Niessen W (1985) Inorg Chem 24:4247
27. Decleva P, Fronzoni G, De Alti G, Lisini A (1988) J Mol Struct Theochem 184:49
28. Decleva P, Fronzoni G, Lisini A (1989) Chem Phys 134:307
29. Böhm MC, Gleiter R, Batich CD (1980) Helv Chim Acta 63:990
30. Böhm MC, Gleiter R (1980) Theor Chim Acta 57:315
31. Böhm MC, Gleiter R (1986) Chem Phys Lett 123:87
32. Moncrieff D, Hillier IH, Saunders VR, von Niessen W (1986) Chem Phys Lett 131:545
33. Ning CG, Hajgato B, Huang YR, Zhang SF, Liu K, Luo ZH, Knippenberg S, Deng JK, Deleuze MS (2008) Chem Phys 343:19

34. Itatani J, Levesque J, Zeidler D, Niikura H, Pépin H, Kieffer JC, Corkum PB, Villeneuve DM (2004) Nature 432:867
35. Pavičić D, Lee KF, Rayner DM, Corkum PB, Villeneuve DM (2007) Phys Rev Lett 98:243001
36. Liebsch T, Plotzke O, Heiser F, Hergenhahn U, Hemmers O, Wehlitz R, Viefhaus J, Langer B, Whitfield SB, Becker U (1995) Phys Rev A 52:457
37. Decleva P, Fronzoni G, Furlan S, Stener M (2001) Chem Phys Lett 348:363
38. Decleva P, Fronzoni G, Stener M, de Simone M, Coreno M, Green JC, Hazari N, Plekan O (2005) Phys Rev Lett 95:263401
39. Yamazaki M, Adachi J, Teramoto T, Yagishita A, Stener M, Decleva P (2009) J Phys B: At Mol Opt Phys 42:051001
40. Yamazaki M, Adachi J, Kimura Y, Stener M, Decleva P, Yagishita A (2010) J Chem Phys 133:164301
41. Goddard R, Krüger C, Mark F, Stansfield R, Zhang X (1985) Organometallics 4:285
42. Casarin M, Pandolfo L, Vittadini A (2001) Organometallics 20:754
43. Gritsenko OV, Braïda B, Baerends EJ (2003) J Chem Phys 119:1937